Involvement of protein kinase C β–extracellular signal-regulating kinase$_{1/2}$/p38 mitogen-activated protein kinase–heat shock protein 27 activation in hepatocellular carcinoma cell motility and invasion

Kun Guo,[1,2] Yinkun Liu,[1,2,3] Haijun Zhou,[1,2] Zhi Dai,[1,2] Jubo Zhang,[1] Ruixia Sun,[1] Jie Chen,[1] Qianglin Sun,[1] Wenjing Lu,[1] Xiaonan Kang[1,2] and Pei Chen[2]

[1]Liver Cancer Institute, Zhongshan Hospital, and [2]Research Center for Cancer, Institute of Biomedical Science, Fudan University, No.180, Fenglin Road, Shanghai 200032, China

(Received June 27, 2007/Revised October 24, 2007/Accepted November 1, 2007/Online publication December 27, 2007)

To understand the molecular mechanism that underlies the role of various prominent signal pathways in hepatocellular carcinoma (HCC) metastasis, a human signal transduction oligonucleotide microarray analysis was carried out in cultured HCC cell models with increasing spontaneous metastatic potential (MHCC97L, MHCC97H, and HCCLM6). The results revealed that the mitogen-activated protein kinase (MAPK) pathway is the prominently upregulated pathway in HCC metastasis. Further study showed that basal phosphorylated levels of extracellular signal-regulating kinase (ERK)$_{1/2}$ and p38 MAPK consecutively increased from MHCC97L to MHCC97H to HCCLM6 cells, but not c-Jun N-terminal kinase. The phosphorylation of ERK$_{1/2}$ and p38 MAPK was regulated by upregulated protein kinase Cβ (PKCβ) in HCC cells through the integrated use of PKCβ RNA interference, the PKCβ specific inhibitor enzastaurin and a PKC activator phorbol-12-myristate-13-acetate. Heat shock protein 27 (HSP27) was also verified as a downstream common activated protein of PKCβ–ERK$_{1/2}$ and PKCβ–p38 MAPK. *In vitro* migration and invasion assay further showed that the depletion of PKCβ or inhibition of PKCβ activation effectively decreased HCC cell motility and invasion. Moreover, the motility and invasion of phorbol-12-myristate-13-acetate-stimulated PKCβ-mediated HCC cells was significantly negated by an ERK inhibitor, 1.4-diamino-2.3-dicyano-1.4-bis[2-aminophenylthio] butadiene, or a p38 MAPK inhibitor, 4-(4-Fluorophenyl)-2-(4-methylsulfinylphenyl)-5-(4-pyridyl)1H-imidazole. It also showed that HSP27 is critical in PKCβ-mediated HCC cell motility and invasion. Taken together, this study reveals the important role of this PKCβ-ERK$_{1/2}$/p38MAPK-HSP27 pathway, which was verified for the first time, in modulating HCC cell motility and invasion. (*Cancer Sci* 2008; 99: 486–496)

HCC is the fourth most common cause of cancer death.[1] Considerable interest has been focused on the mechanisms of HCC tumorigenesis and metastasis, the most fundamental characteristics of cancer and the ultimate cause of most cancer mortality.[2,3] For tumor cells, the ability to metastasize might depend on the alteration of a series of signal transduction networks that enables them to complete all the steps of metastatic cascade.[4,5] These alterations of cell signaling are often due to an increase in the activities of signal molecules, their regulation at the transcriptional level, and their post-translation modification, especially in protein phosphorylation.[6–8] At present, a series of human HCC cell lines with different metastatic potentials have been established at the authors' institute,[9,10] supplying a research platform for better insight into the mechanisms of human HCC metastasis. Two different metastatic HCC cell clones, MHCC97L and MHCC97H, were isolated from the same parent cell line MHCC97, derived from a nude mice model of human HCC metastasis (LCI-D20). Spontaneous pulmonary metastasis occurred in 40% and 100% of recipient nude mice after orthotopic transplantation of MHCC97L and MHCC97H, respectively. HCCLM6 was selected after MHCC97H had completed six rounds of lung metastasis *in vivo* and produced further multiple extensive metastasis through both blood vessels and lymphatic channels. These cell lines make our HCC metastatic cells a unique study model system, in that they are all derived from the same parent cell, thus having a similar genetic background yet with dramatic differences in spontaneous metastatic behaviors. Such characteristics make these cell lines have good value for comparative study.

In order to understand the molecular mechanisms of specific signal transduction pathways responsible for human HCC metastasis, a human signal transduction oligonucleotide microarray analysis was carried out to compare gene expression patterns in metastatic MHCC97L, MHCC97H, and HCCLM6 cells. Analysis of the microarray data revealed prominent roles for the MAPK pathway during human HCC metastasis, confirmed by further biochemical and functional investigation.

Materials and Methods

Cell lines. Three human HCC cell lines, MHCC97L, MHCC97H,[10] and HCCLM6,[9] were cultured at 37°C in 5% CO_2 in DMEM (Gibco BRL, Grand Island, NY) supplemented with 10% fetal calf serum (Hyclone, UT). Briefly, the cells were grown to 90% confluency and harvested by treating with 0.25% trypsin and 0.02% EDTA. Cells were rinsed three times with phosphate-buffered saline and centrifuged for further RNA isolation and protein extraction.

RNA isolation and cDNA array hybridization. Total RNA was extracted from cells using Trizol reagent (Invitrogen, MD). Further affinity column purification of total RNA was carried out by NucleoSpin RNA clean-up kit (Macherey-Nagel, Germany). Analysis of signal transduction molecules was carried out using Human Signal Transduction Oligo array (CapitalBio, Beijing, China). Each chip contained triplicate spots of oligo fragments of 909 genes, including four human housekeeping gene oligonucleotides

[3]To whom correspondence should be addressed. E-mail: liu.yinkun@zs-hospital.sh.cn
Abbreviations: EDTA, ethylenediaminetetraacetic acid; ERK, extracellular signal-regulating kinase; DMEM, Dulbecco's modified Eagle's medium; FDR, false discovery rate; GAPDH, glyceraldehyde-3-phosphate dehydrogenase; HCC, hepatocellular carcinoma; HSP27, heat shock protein 27; JNK, c-Jun N-terminal kinase; LY317615, enzastaurin; MAPK, mitogen-activated protein kinase; MTT, 3-(4,5-dimethylthiazol-2-yl)-2,5-diphenyltetrazolium bromide; PKCβ, protein kinase Cβ; PMA, phorbol-12-myristate-13-acetate; SB203580, 4-(4-Fluorophenyl)-2-(4-methylsulfinylphenyl)-5-(4-pyridyl)1H-imidazole; RNAi, RNA interference; SDS, sodium dodecyl sulfate; siRNA, small interfering RNA; SP600125, 1,9-pyrazoloanthrone; SSC, standard saline citrate; U0126, 1.4-diamino-2.3-dicyano-1.4-bis[2-aminophenylthio] butadiene.

doi: 10.1111/j.1349-7006.2007.00702.x

used as positive controls and for data normalization, eight non-human genes used as negative controls, and 897 genes with functions related to cell signaling. The list of genes is available online at http://www.qiagen.com/catalog/auto/cget.asp?p = microarray_products. From each cell line, 5 μg total RNA was converted into cDNA and labeled with Cy3 or Cy5 using the CapitalBio cDNA array labeling kit. DNA in hybridization solution (3 × SSC, 0.2% SDS, 5 × Denhardt's solution, and 25% formamide) was denatured at 95°C for 3 min prior to loading onto a microarray. Arrays were hybridized at 42°C overnight and washed with two consecutive solutions (0.2% SDS and 2 × SSC at 42°C for 5 min, and 0.2 × SSC for 5 min) at room temperature. Following hybridization, the chips were washed and then scanned with a LuxScan 10KA double pathway laser scanner to obtain high-resolution images of 16 bits in tiff format. For the total RNA from each cell line, Cy3–Cy5 exchange labeling was necessary for accurate results and to meet the objectives of the experiment.

Data processing and clustering. Signal intensities of individual spots from the 16-bit tiff images were quantified using GenePix Pro 4.0. As a measurement of technical replication, one swap-dye experiment was carried out on each biological sample so that a total of six data points were available for a gene on the microarrays. The linear normalization method based on the expression levels of four human housekeeping genes in combination with the yeast external controls was used for data analysis. Normalized data was log transformed; microarray spots in the *t*-test, if combined with ratio values of expressed genes with 1.5-fold difference, were regarded as significantly different. Hierarchical clustering with the average linkage method was used on those genes that passed the *t*-test and the cluster data was visualized using the Treeview program.

Identification of metastasis-associated signal pathways. KOBAS software was used to identify biochemical pathways involved in increasing metastatic potential and to calculate the statistical significance of each pathway.[11,12] KOBAS assigns a given set of genes to pathways by first matching the genes to similar genes in known pathways in the KEGG database. We also manually reviewed all identified pathways for quality control. As a large number of pathways are involved, FDR correction was implemented to control the overall Type I error rate of multiple hypotheses testing using GeneTS (2.8.0) in the R (2.2.0) statistics software package. Pathways with FDR-corrected P-values < 0.05 were considered statistically significant.

PKC inhibition assays. The inhibition of PKCα, PKCβ, PKCγ, or PKCδ activity by LY317615 was determined using the HTScan PKC Kinase Assay Kit from Cell Signaling Technology (Beverly, MA). Briefly, reactions were carried out in 50 μL reaction volumes in 96-well polystyrene plates with final conditions as follows: 25 mM Tris-HCL (pH 7.5), 10 mM $MgCL_2$, 5 mM β-glycerophosphate, 0.1 mM $NaVO_3$, 2 mM dithiothreitol, 200 μM adenosine 5'-triphosphate, 1.5 μM substrate peptide, serial dilutions of LY317615 (0, 0.025, 0.05, 0.1, 1, 2.5, and 10 μM), and recombinant human PKCα, PKCβ, PKCγ, or PKCδ enzymes (10, 10, 10, or 50 ng, respectively). Reactions were started with enzyme addition, incubated at room temperature for 15 min, then add 50 μL/well stop buffer (50 mM EDTA, pH 8.0) was added to stop the reaction. Twenty-five microliters of each reaction was transferred to a 96-well streptavidin-coated plate containing 75 μL dH_2O/well and incubated at room temperature for 60 min. The plate was washed and incubated with 100 μL/well phosphor-PKA substrate (RRXS/T) (100G7) rabbit primary antibody at 37°C for 120 min, then washed again and europium-labeled secondary antibody was added at room temperature for 30 min. After incubation with DELFIA enhancement solution for 5 min, plates were read on a time-resolved plate reader.

Immunoblot analysis. Equal amounts of protein extracts in SDS–lysis buffer containing phosphatase inhibitor cocktail were subjected to 12% SDS–polyacrylamide gel electrophoresis analysis then electrophoretically transferred to a polyvinylidene difluoride membrane using a Bio-Rad Semi-Dry apparatus. After blocking with blocking buffer (1 × Tris-buffered saline and 0.05% Tween-20 with 5% non-fat dry milk or 5% bovine serum albumin) for 1 h, the membranes were probed with different antibodies against PKCβ (Biosciences Pharmingen, USA), phosphor-PKCβ (Thr500; Upstate Biotechnology, NY, USA), HSP27 and phosphor-HSP27 (ser82; Cell Signaling Technology), p38 MAPK, phosphor-p38, $ERK_{1/2}$, phosphor-$ERK_{1/2}$, JNK, and phosphor-JNK overnight at 4°C. The membrane was incubated with horseradish peroxidase-conjugated secondary antibody for 1 h at room temperature. An enhanced chemiluminescence system (Pierce Biotechnology, Rockford, IL) was used for detection. Relative band intensities were determined by quantization of each band with an Imagemaster system.

RNA interference. siRNA specifically targeting HSP27 (sense, 5′-ACGGUC AAGACCAAGGAUGdTdT-3′; antisense, 5′-CAU-CCUUGGUCUUGACCGUdTdT-3′) was purchased from Cell Signaling Technology and three siRNAs targeting PKCβ were constructed and chemically synthesized. PKCβ siRNA-1: sense 5′-GCCAGUGUUGAUGGCUGGUdTdT-3′; antisense, 5′-ACCA-GCCAUCAACACU GGCdTdT-3′; PKCβ siRNA-2: sense, 5′-GUGAGGCCAAUGAAGAACUdTd T-3′; antisense, 5′-AGUUCU-UCAUUGGCCUCACdTdT-3′; and PKCβ siRNA-3: sense, 5′-GCCAGUGUUGAUGGCUGGUdTdT-3′; antisense, 5′-ACCAGC-CAUCAACACU GGCdTdT-3′. The siRNAs were evaluated for sequence specificity by a BLAST search and did not show homology to other known genes. Non-silencing control siRNA duplexes (sense, 5′-UUCUCCGAACGUGUCACGUdTdT-3′; antisense, 5′-ACGUGACACGUUCGGAGAAdTdT-3′) were synthesized using scrambled sequences as a negative control to assay the efficiency of interference of PKCβ siRNA. Briefly, 24 h prior to transfection, cells were seeded in 6-well plates at a density of 2×10^5 cells/well. siRNA molecules were transfected with a final concentration of 100 nM for HSP27 and 70 nM for PKCβ using Lipofectamine 2000 reagent (Invitrogen) according to the manufacturer's instructions. Lysates were prepared after 36–48 h in lysis buffer and equal amounts of RNA and protein were subjected to immunoblot analysis.

***In vitro* invasion assay.** *In vitro* invasion assay was carried out using a 24-well Transwell unit with polycarbonate filters. Briefly, 24 h after plating, cells were pretreated with LY317615 (0.025 μM), U0126 (10 μM), SB203580 (5 μM), or PMA (20 nM) prior to the invasion assay. Cells were detached by treatment with trypsin/EDTA, washed, resuspended in DMEM cell culture media (Gibco BRL) with 0.1% bovine serum albumin, and 3×10^5 cell suspensions were placed into the upper chamber of a 24-well chamber unit (i.e. 105 cells/well). Cells were allowed to invade for 17 h through a polycarbonate membrane coated with Matrigel, a reconstituted basement membrane gel, towards serum-free NIH-3T3 conditioned medium present in the lower chamber as a source of chemoattractants. The membrane were fixed with methanol, and stained with Giemsa for 10 min. Cells in the upper chamber were removed by cotton swab and the cells that invaded through the Matrigel and were located on the underside of the filter (16 fields/filter) were counted. Three invasion chambers were used per condition. The values obtained were calculated by averaging the total number of cells from three filters.

***In vitro* migration assay.** *In vitro* migration assay was carried out using a 24-well Transwell unit with polycarbonate filters. Experimental procedures were the same as the *in vitro* invasion assay described above except that the filter was not coated with Matrigel for the migration assay.

MTT assay. Cell viability was assayed by the MTT (Sigma) method. Briefly, 5×10^3 cells in 160 μL medium were seeded to each well of a 96-well microtiter plate (three wells/dose). After cell attachment, specific compounds with prescriptive concentrations were incubated for the indicated time points. At the end of the

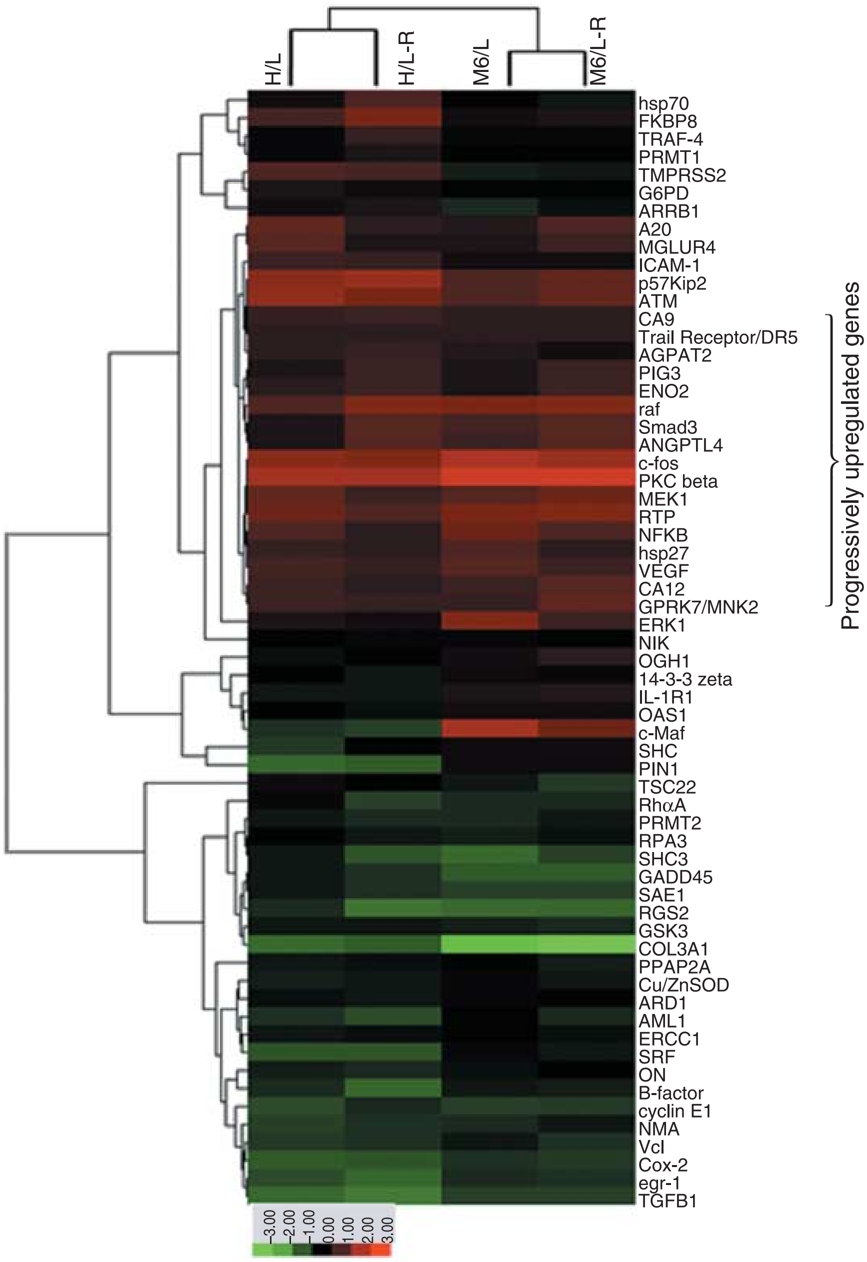

Fig. 1. Clustering analysis of differently expressed genes in three hepatocellular carcinoma cell lines. Hierarchical clustering was carried out using Pearson's correlation distance and averaging linkage of cell lines and genes. Each row represents one of 62 differently expressed genes; each column represents a separate swap-dye experiment. High and low expression are shown in red and green, respectively. –R, reverse-dye experiment.

treatment, the medium was replaced with 100 µL phenol red-free medium containing 0.5 mg/mL MTT. Cells were incubated for a further 4 h. The MTT medium was then replaced with 100 µL dimethylsulfoxide, and the absorbance of each well was measured at 540 nm with a micro-enzyme-linked immunosorbent assay reader.

Statistical analysis. Data were expressed as mean ± SEM and analyzed using ANOVA. Student's *t*-test was used in two-group comparisons. The association between the various factors was determined using Pearson's correlation. $P < 0.05$ was considered to be statistically significant.

Results

Identification of 17 genes with preferentially upregulated expression in metastatic HCC cells. To investigate the expression patterns of signal transduction-related genes in MHCC97L, MHCC97H, and HCCLM6 cells, a human signal transduction oligo microarray was used including 897 genes with functions related to cell signal transduction pathways. A total of 62 statistically and consecutively changed genes passed the statistic *t*-test, if combined with ratio values of 1.5-fold difference, among which 17 genes showed step-wise upregulation. These gradually upregulated genes were extracted from the clustering (Fig. 1). The resulting final group, containing 17 genes that showed upregulated expression from MHCC97L to MHCC97H to HCCLM6 cell lines, are presented in Table 1.

Several signal transduction pathways significantly upregulated during HCC cell metastatic potential development. All genes on the microarray were analyzed using KOBAS,[11,12] to identify the signal transduction pathways in which they function. KOBAS mapped 897 genes to 142 KEGG pathways, including 62 consecutively-changed genes to 66 pathways and 17 upregulated genes to 34 pathways. Fourteen of the latter 34 pathways were significantly upregulated ($P < 0.05$) and associated with HCC cell metastasis if judged by P-values based on hypergeometric distribution. Only three of these pathways

doi: 10.1111/j.1349-7006.2007.00702.x

Table 1. Consecutively upregulated genes with over 1.5-fold difference in three hepatocellular carcinoma cell lines with increasing metastatic potentials

Gene symbol	Fold (H/L)	Fold (M6/L)	GenBank Accession No.	Description
PRKCB1	3.6664	5.1265	M13975	Protein kinase C, beta 1
FOS	2.9141	3.6328	V01512	V-fos FBJ murine osteosarcoma viral oncogene homolog
RAF1	2.4416	2.7255	X03484	V-raf-1 murine leukemia viral oncogene homolog 1
NDRG1	2.2842	2.6985	NM_006096	N-myc downstream regulated gene 1
MAP2K1	2.0016	2.2717	NM_002755	Mitogen-activated protein kinase kinase 1
NFKB1	1.8207	2.1803	M58603	Nuclear factor of kappa light polypeptide gene enhancer in B-cells 1 (p105)
MADH3	1.7797	2.0065	NM_005902	MAD, mothers against decapentaplegic homolog 3
VEGF	1.7681	1.9607	NM_003376	Vascular endothelial growth factor
ANGPTL4	1.7176	1.9527	NM_016109	Angiopoietin-like 4
GPRK7	1.6996	1.9335	NM_017572	G protein-coupled receptor kinase 7
CA12	1.6292	1.8924	NM_001218	Carbonic anhydrase XII
HSPB1	1.5856	1.7717	NM_001540	Heat shock 27 kDa protein 1
CA9	1.5656	1.7391	NM_001216	Carbonic anhydrase IX
PIG3	1.5492	1.6925	NM_004881	Quinone oxidoreductase homolog
ENO2	1.5415	1.6412	NM_001975	Enolase 2 (gamma, neuronal)
AGPAT2	1.5258	1.5825	NM_006412	1-Acylglycerol-3-phosphate-acyltransferase 2
TNFRSF10B	1.5008	1.5385	AF016266	Tumor necrosis factor receptor superfamily, member 10b

H, MHCC97H; L, MHCC97L; M6, HCCLM6.

Table 2. Representative preferential signal pathways associated with metastasis in hepatocellular carcinoma cell lines identified by KOBAS[11,12] †

KEGG pathways	No. of genes located in various pathways	No. of consecutively upregulated genes	*P*-value	FDR-corrected *P*-value
Mitogen-activated protein kinase signaling pathway	262	6	7.325e-06	0.00025
Nitrogen metabolism	24	2	0.00112	0.01911
Natural killer cell-mediated cytoxicity	143	3	0.00290	0.03293
Focal abhesion	211	3	0.00859	0.05413
Long-term potentiation	68	2	0.00857	0.05413
Long-term depression	78	2	0.01114	0.05413
B-cell receptor signaling pathway	74	2	0.01007	0.05413
Apotosis	98	2	0.01718	0.05518
T-cell receptor signaling pathway	93	2	0.01556	0.05518
Toll-like receptor signaling pathway	100	2	0.01785	0.05518
Gap junction	99	2	0.01751	0.05518
Phenylalanine, tyrosine, and tryptophan biosynthesis	12	1	0.02474	0.07009
Insulin signaling pathway	138	2	0.03251	0.08504
Wnt signaling pathway	145	1	0.03560	0.08646

†Seventeen consecutively upregulated genes involved in 34 pathways. The pathways include: dorso-ventral axis formation; phosphatidylinositol signaling system; cytokine–cytokine receptor interaction; Fc epsilon RI signaling pathway; glycolysis/gluconeogenesis; adipocytokine signaling pathway; glycerolipid metabolism; glycerophospholipid metabolism; adherens junction; protein folding and associated processing; transforming growth factor-β signaling pathway; tight junction; leukocyte transendothelial migration; cell cycle; CAM ligands; calcium signaling pathway; cytokine receptors; regulation of actin cytoskeleton; cytokines; and CD molecules. FDR, false discovery rate.

had *P*-values < 0.05 after FDR correction. The MAPK pathway ranked number one with an FDR-corrected *P*-value of 0.00025 (Table 2). This pathway was the focus for further experiments.

$ERK_{1/2}$ and p38 MAPK pathways constitutively active in three metastatic HCC cell lines. Current evidence suggests mammalian cells express at least three groups of MAPKs: ERKs; p38 MAPKs; and JNKs. Each is pivotal and representative of signal molecules involved in different MAPK pathways.[13,14] To further verify the consistent activation of the particular MAPK pathways in the three cell lines, we observed the levels of these three molecules and their phosphorylation through immunoblot analysis. The results showed that both $ERK_{1/2}$ and phosphor-$ERK_{1/2}$ were consecutively overexpressed and the basal ratio of phosphorylation also increased step-wise from MHCC97L to MHCC97H to HCCLM6 cells. Although total p38 MAPK did not change, its phosphorylation showed significantly elevated levels in these cell lines. For JNK and phosphor-JNK, protein levels did not change (Fig. 2).

PKCβ activity influences ERK1/2 and p38 MAPK phosphorylation in HCC cells. It is well-recognized that PKC is an upstream regulator of the Raf-1-MEK1/2-p44/p42 MAPK cascade.[15] Our microarray data showed consecutively marked upregulation of PKCβ in HCC cells. Thus, we investigated whether PKCβ is activated in HCC cells. The result showed the basal level of PKCβ phosphorylation increased from MHCC97L to MHCC97H to HCCLM6 cells (Fig. 2). To elucidate whether PKCβ is involved in the activation of MAPK pathways in these cells, we examined the effect of LY317615, recently identified as an inhibitor of PKCβ,[16] on the basal levels of $ERK_{1/2}$, p38MAPK, and JNK phosphorylation. Because it was reported that high concentrations of LY317615 could inhibit other PKC isoforms,[17] we verified that 0.025 μM LY317615 specifically inhibited phosphor-PKCβ, and not other PKC isoforms, through PKC inhibition assay (Fig. 3a). It was further observed that phosphor-ERK and phosphor-p38 decreased after treatment with

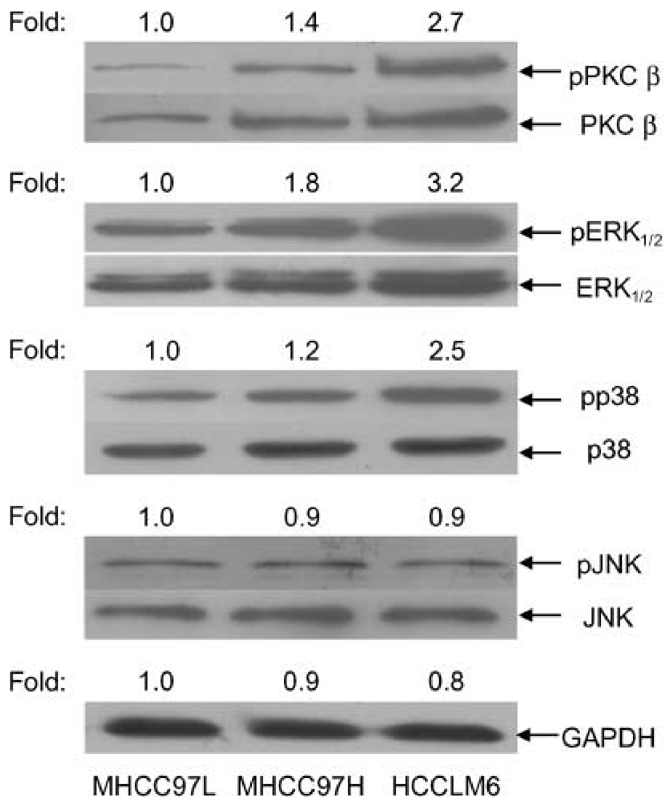

Fig. 2. The extracellular signal-regulating kinase (ERK)$_{1/2}$ pathway, p38 mitogen-activated protein kinase (MAPK) pathway, and protein kinase Cβ (PKCβ) were consecutively activated in metastatic hepatocellular carcinoma cell clones MHCC97L, MHCC97H, and HCCLM6. The levels of ERK$_{1/2}$, p38 MAPK, c-Jun N-terminal kinase, and PKCβ and their basal phosphorylation were determined by immunoblot analysis of whole cell lysate (30 µg) using specific and phosphospecific antibodies. The values on top of the bands represent the densitometric estimation of the relative density of the band, calculated by comparing the ratio of phosphor-protein *versus* total protein intensity of MHCC97H and HCCLM6 cell lines with that of MHCC97L cell line (the ratio in MHCC97L was set as baseline 1.0). The level of glyceraldehyde-3-phosphate dehydrogenase served as the loading control.

0.025 µM LY317615, whereas phosphor-JNK was unchanged (Fig. 3b).

It is well-known that both classical and novel PKC are directly activated by phorbol-esters such as PMA.[18] To further investigate the effect of PKCβ activation on ERK$_{1/2}$ and p38 MAPK in HCC cells, we designed three different siRNAs targeting distinct parts of PKCβ mRNA to specifically deplete PKCβ in HCC cells. These siRNAs were then transfected into HCC cells. As Fig. 3c shows, PKCβ siRNA-1 had the highest interference efficiency of the three siRNAs, but expression of GAPDH was not affected. PKCβ siRNA-1 was chosen for the following experiments. We treated HCC cells with PKCβ siRNA-1 followed by PMA stimulation and the result showed that PMA stimulation alone significantly strengthened the phosphorylation levels of ERK$_{1/2}$ and p38MAPK. However, phosphor-ERK$_{1/2}$ and phosphor-p38 MAPK decreased after PKCβ RNAi followed by PMA stimulation in HCC cells, compared with PMA-treated HCC cells (Fig. 3d).

HSP27 is a cross-talk molecule downstream of PKCβ–ERK$_{1/2}$ and PKCβ–p38 MAPK pathways in HCC cells. It has been reported that HSP27 was originally discovered as a modulator of actin polymerization and reorganization, whose function is phosphorylation-dependent.[19,20] We analyzed the levels of HSP27 and it's phosphorylation in MHCC97L, MHCC97H, and HCCLM6 cells. As shown in Fig. 4a, HSP27 expression was constitutively upregulated in the three cell lines, consistent with the results from the gene microarray, and the basal phosphorylation level was step-wisely increased.

It is also recognized that HSP27 phosphorylation is catalyzed by the MAPK superfamily.[21–23] It has been found in our study that ERK$_{1/2}$ and p38 MAPK were constantly activated in HCC cells. To elucidate whether MAPKs are involved in the phosphorylation of HSP27 in HCC cells, we examined the effect of U0126 (a specific inhibitor of ERK$_{1/2}$), SB203580 (a specific inhibitor of p38 MAPK), and SP600125 (a specific inhibitor of JNK) on the phosphorylation levels of HSP27. Although U0126 and SB203580 suppressed the phosphorylation of HSP27, the basal levels of total HSP27 were not affected, and SP600125 did not inhibit phosphor-HSP27 or total HSP27 (Fig. 4b).

Moreover, it was found that the PKCβ-specific inhibitor LY317615 also suppressed the phosphorylation level of HSP27 (Fig. 3b). To further investigate the effect of PKCβ activation on the phosphorylation of HSP27 through ERK$_{1/2}$ and p38 MAPK, we treated HCC cells with U0126 for 1.5 h or SB203580 for 2 h, followed by PMA stimulation for 4 h, and examined phosphor-HSP27 levels in cell protein extracts. Compared with PMA stimulation alone, the phosphorylation level of HSP27 was reduced in HCC cells treated with U0126 or SB203580 followed by PMA stimulation (Fig. 4c).

PKCβ–ERK$_{1/2}$/p38 MAPK–HSP27 involved in HCC cell invasion and motility. These observations revealed the upregulation of the PKCβ–ERK$_{1/2}$/p38 MAPK–HSP27 pathway activation in different metastatic HCC cells and prompted us to show whether the pathway was directly related to HCC cells' metastatic phenotype. Firstly, we treated HCC cells with inhibitor LY317615. As shown by the *in vitro* migration and invasion assays, the motility and invasion abilities of HCC cells were reduced with the inhibition of PKCβ activity (Fig. 5a). This reduction was also confirmed by treating HCC cells with PKCβ-specific siRNA-1 (Fig. 5b). To rule out the possibility of off-target effects that might create false-positive results, the knockdown experiment was replicated using a second independent siRNA-3 for PKCβ depletion. The observation also verified the reduction in the number of HCC cells passing through chamber membranes (Fig. 5c). These results revealed the specificity of PKCβ RNAi.

To investigate further the prominent role of PKCβ, compared with other PKC isozymes, in HCC metastasis, HCCLM6 cells were transfected with PKCβ-specific siRNA-1, then treated with PKC activator PMA (20 nM). Compared with PMA stimulation alone, the motility and invasion ability of HCC cells treated with PKCβ RNAi then PMA was significantly reduced. There was no statistical difference *versus* independently PKCβ RNAi-treated cells (Fig. 5d,e).

In addition, to observe the effects of ERK$_{1/2}$, p38 MAPK, and HSP27 activation on PMA-stimulated HCC cells' motility and invasion, we treated HCC cells with SB203580 or U0126 followed by PMA stimulation. As shown in Fig. 6a–d, such treatment significantly decreased basal phosphorylation levels of ERK$_{1/2}$ and p38 MAPK and reduced the numbers of migrated and invasive HCC cells. However, SB203580 and U0126 barely decreased the phosphorylation of PMA-stimulated PKCβ (Fig. 6e). This indicates that, in HCC cells, neither SB203580 nor U0126 inhibited the phosphorylation of PKCβ. Moreover, we knocked down HSP27 expression in HCC cells with specific siRNA,[24] (Fig. 6f) followed by PMA stimulation, and analyzed HCC cell motility and invasive ability. This experiment also showed that HCC cell invasion and motility were significantly decreased (Fig. 6g).

To establish whether these results were from toxicity of LY317615 and PMA, or depletion of PKCβ protein or HSP27 protein, cell survival was determined by MTT assay. A decrease in cell survival rates was not notably shown in LY317615- or PMA-treated HCC cells (Fig. 6h). PKCβ RNAi-treated or HSP27

doi: 10.1111/j.1349-7006.2007.00702.x

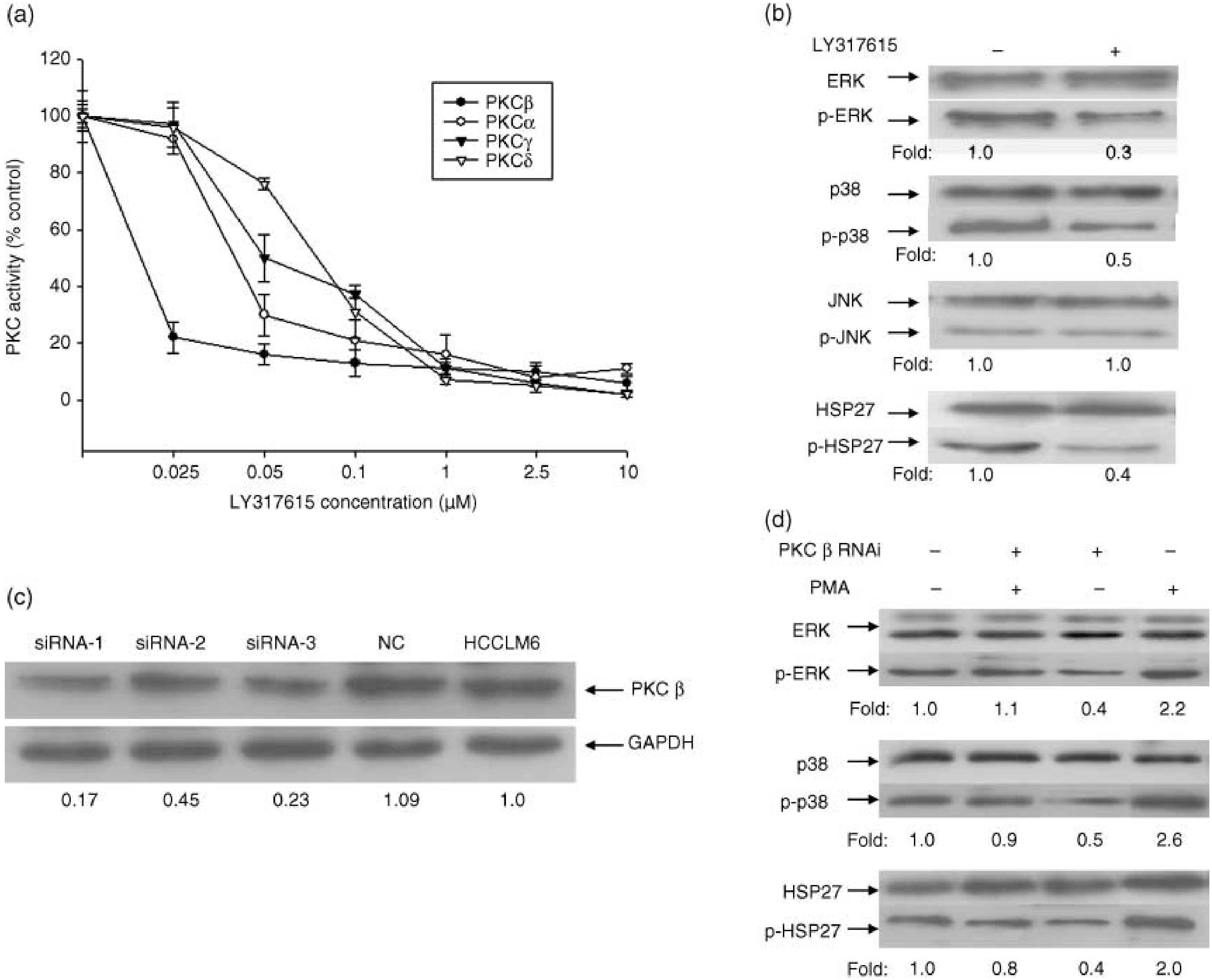

Fig. 3. Extracellular signal-regulating kinase (ERK)$_{1/2}$ and p38 mitogen-activated protein kinase (MAPK) pathways were efficiently activated by upstream protein kinase Cβ (PKCβ) in hepatocellular carcinoma (HCC) cells. (a) PKC inhibition assays with a series concentration of enzastaurin (LY317615; 0, 0.025, 0.05, 0.1, 1, 2.5, and 10 μM) were carried out in HCC cells the using HTScan PKC Kinase Assay Kit from Cell Signaling Technology (Beverly, MA). Inhibition of PKCα, PKCβ, PKCγ, or PKCδ by various concentrations of LY317615 was determined through detecting fluorescence values of reaction solutions. The fluorescence value of reaction solution with 0 μM LY317615 served as a percent control for each PKC inhibition assay. (b) HCCLM6 cells pretreated with 0.025 μM LY317615 for 1.5 h and the cell extracts (20 μg) were subjected to sodium dodecyl sulfate–polyacrylamide gel electrophoresis (SDS-PAGE), the levels of ERK$_{1/2}$, p38 MAPK, c-Jun N-terminal kinase, heat shock protein 27 (HSP27), and their phosphorylation were determined by immunoblot analysis. The values underneath the bands represent the densitometric estimation of the relative density of the band, calculated by comparing the ratio of phosphor-protein *versus* total protein intensity of LY317615-treated HCCLM6 cells with that of HCCLM6 cells without LY317615 treatment (the ratio in HCCLM6 cells without LY317615 treatment was set as baseline 1.0). Similar findings were also observed in metastatic HCC cell clones MHCC97L and MHCC97H (data not shown). (c) HCCLM6 cells were transfected with PKCβ small interfering RNA (siRNA)-1 (70 nM), siRNA-2 (70 nM), siRNA-3 (70 nM), and negative control (non-specific siRNA) for 48 h. Equal amounts of cell extracts (30 μg) were subjected to SDS-PAGE, and the levels of total PKCβ were determined by immunoblot analysis. The level of glyceraldehyde-3-phosphate dehydrogenase (GAPDH) served as the loading control. The values underneath the bands represent the densitometric estimation of the relative density of the band, calculated by comparing the ratio of PKCβ *versus* GAPDH with that of HCCLM6 cells without siRNA treatment (the ratio in HCCLM6 cells without siRNA treatment was set as baseline 1.0). (d) After HCCLM6 cells were transfected with PKCβ siRNA-1 (70 nM) followed by phorbol-12-myristate-13-acetate (20 nM) for 4 h, levels of phosphor-ERK$_{1/2}$, phosphor-p38 MAPK, phosphor-HSP27, and total proteins were estimated. The values underneath the bands represent the relative ratios of phosphorylation *versus* total protein compared with that of HCCLM6 cells. Similar findings were also observed in MHCC97L and MHCC97H cells (data not shown).

RNAi-treated cells' survival rates reduced by 6% in 48 h and 12% in 36 h, respectively, while the decrease in cell motility and invasion in the same time periods was 53% and 57% (Fig. 5b), and 63% and 71%, respectively (Fig. 6g). It therefore seems that the depletion of PKCβ or HSP27 is the main cause of decreased levels of HCC cell motility and invasion.

Discussion

In this study, we found that the consecutive activation of two MAPK pathways played an important role in human HCC cell motility and invasion through integrated genomic, molecular biological, and functional studies. Although it is still unclear

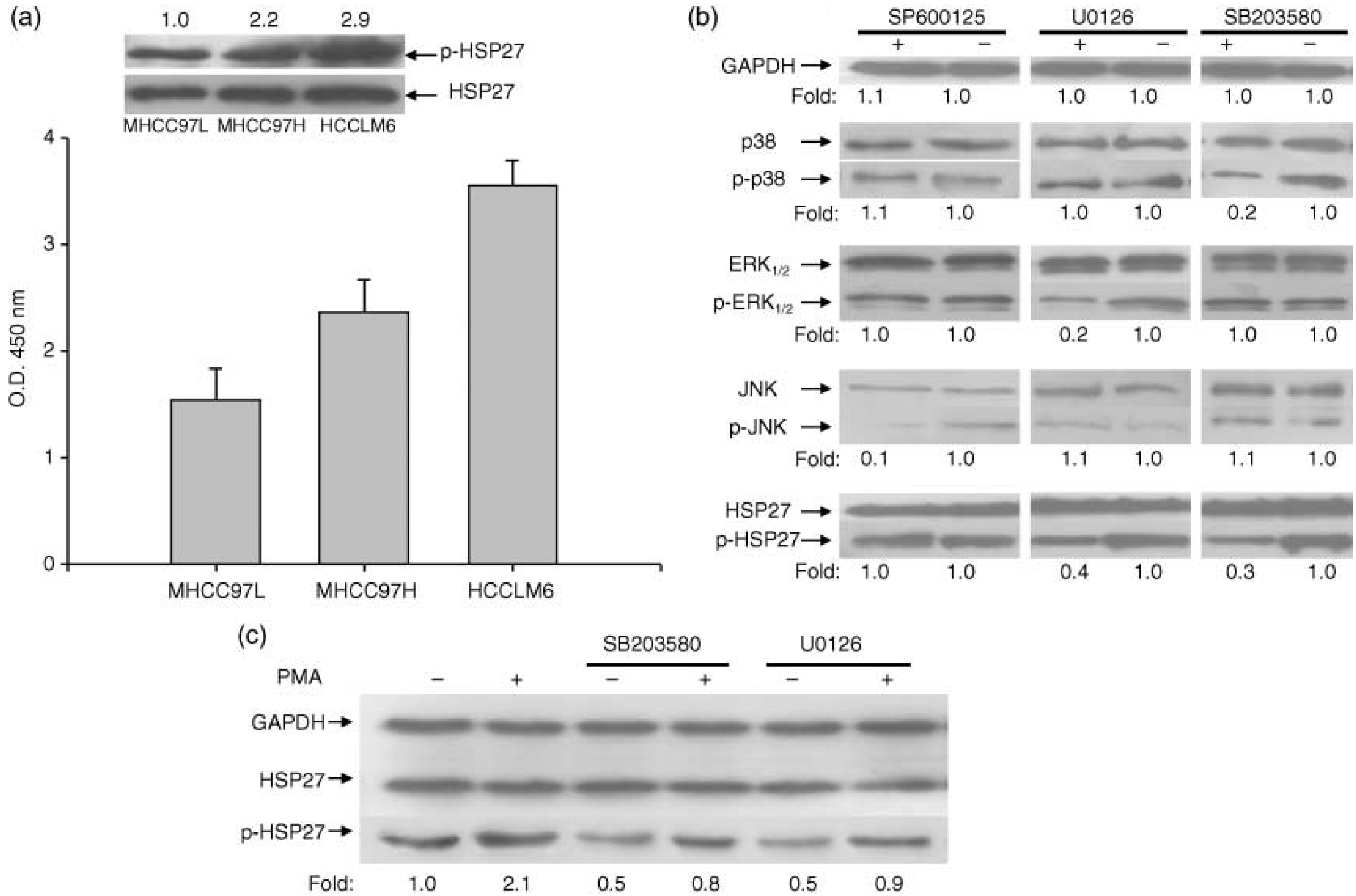

Fig. 4. Phosphorylation of heat shock protein 27 (HSP27) was regulated by protein kinase Cβ (PKCβ)–extracellular signal-regulating kinase (ERK)$_{1/2}$ and PKCβ–p38 mitogen-activated protein kinase (MAPK) in hepatocellular carcinoma (HCC) cells. (a) Expression of total HSP27 was analyzed using the BioSource Human HSP27 kit. Equal amounts of total protein, each at a final concentration of 50 μg/mL, from metastatic HCC cell clones MHCC97L, MHCC97H, and HCCLM6 were analyzed using the BioSource Human HSP27 kit and expression of total HSP27 was consecutively increased. Basal phosphorylated level of HSP27 was detected by immunoblot analysis in three HCC cell lines. The values on top of the bands represent the relative ratio of basal phosphorylation in MHCC97L, MHCC97H, and HCCLM6 cells. (b) HCCLM6 cells were treated with 4-(4-Fluorophenyl)-2-(4-methylsulfinylphenyl)-5-(4-pyridyl)1H-imidazole (SB203580; 5 μM) for 2 h, 1.4-diamino-2.3-dicyano-1.4-bis[2-aminophenylthio] butadiene (U0126; 10 μM) for 1.5 h, or 1,9-pyrazoloanthrone (SP600125; 10 μM) for 2 h. Expression of total ERK$_{1/2}$, p38 MAPK, c-Jun N-terminal kinase, HSP27 and their phosphorylated forms were analyzed using specific antibodies by immunoblot analysis. The values underneath the bands represent the ratios of phosphorylation *versus* total proteins of molecules above and show specificity of kinase inhibitors. (c) HCCLM6 cells were pretreated with U0126 (10 μM) for 1.5 h or SB203580 (5 μM) for 2 h followed by phorbol-12-myristate-13-acetate (20 nM) for 4 h. The blots were analyzed using a specific antibody against HSP27 and phosphor-HSP27. The values underneath the bands represent the densitometric estimation of the relative density of the phosphorylated bands *versus* total protein bands compared with that of HCCLM6 cells without treatment. These same findings were also observed in MHCC97L and MHCC97H cells (data not shown).

whether upregulated activity of these MAPK pathways is the initiator or the receiver of elevated malignant potential in human HCC cells, the exact effect of MAPK pathways on HCC cell motility and invasion has been verified in this study.

The MAPK signaling pathways have multiple roles in natural processes such as cell growth, differentiation, and cytoskeleton dynamics.[25–27] The molecular events in which MAPKs function can be separated in discrete and yet interrelated steps: activation of the MAPK by their upstream kinases; changes in the subcellular localization of MAPKs; and recognition, binding, and phosphorylation of MAPK downstream targets. Many studies have identified that constitutive activation of the MAPK signal pathway is common in tumor invasion and metastasis.[26,28–30] Despite these studies on the effects of various manipulations, including growth factors, some kinases, and chemical modifiers in HCC,[31–33] the structure and function of the MAPK pathways in HCC metastasis are far from clearly understood. In this report, our microarray data analysis reveals a prominent role of the MAPK pathway in HCC metastasis, furthermore, several lines of biological and functional evidence suggests an important role for the PKCβ–ERK$_{1/2}$/p38 MAPK–HSP27 pathway in HCC cell motility and invasion.

The results showing step-wise increased basal levels of phosphor-ERK$_{1/2}$ and phosphor-p38 MAPK in three HCC cell lines with different metastatic potentials indicate the constant activation of the ERK$_{1/2}$ and p38 MAPK pathway in HCC, consistent with reports of the pathway's participation in the metastasis of some cancers.[13,34,35] However, upregulation of c-Jun NH2-terminal kinase pathway activation was not found in our HCC cell lines. It indicates that the aberrant regulation of different MAPK cascades might contribute to the resulting pattern of different cancer cell functions.

It is well-recognized that MAPK families are regulated by MAPK kinase kinase–MAPK kinase–MAPK phosphorelay systems in vertebrates.[36] Recently, some hot-point studies have focused on how PKCβ collaborates with MAPK signaling pathways to regulate cell survival and cell death.[37,38] Moreover, the role of PKCβ in carcinogenesis has been recognized.[39,40] It not only accounts for increased invasion and proliferation rates of intestinal

doi: 10.1111/j.1349-7006.2007.00702.x

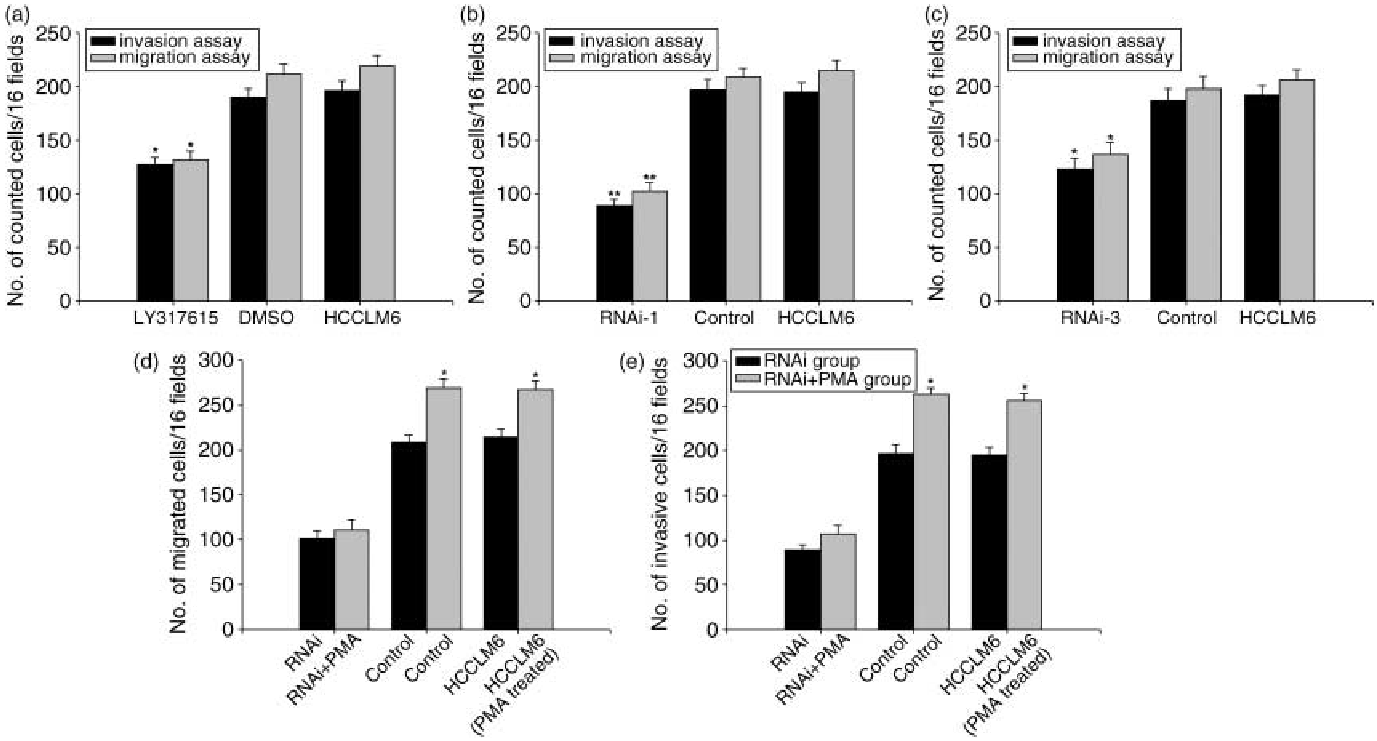

Fig. 5. Protein kinase Cβ (PKCβ)-mediated hepatocellular carcinoma cell motility and invasion. (a) HCCLM6 cells pretreated with 0.025 μM enzastaurin (LY317615) for 1.5 h were subjected to *in vitro* migration and invasion assays for 20 h. The results represent means of three experiments. $^{*}P < 0.05$ *versus* control (dimethylsulfoxide). (b) After HCCLM6 cells were transfected with PKCβ small interfering RNA (siRNA)-1 (70 nM) for 24 h, these cells were then subjected to *in vitro* migration and invasion assays for 20 h. The results represent means of three experiments. $^{**}P < 0.01$ *versus* control (non-specific siRNA). (c) To rule out the possibility of off-target effects, the number of migrated and invasive HCCLM6 cells, which were pretreated with PKCβ siRNA-3 (70 nM) for the same indicated time as with PKCβ siRNA-1, was estimated by carrying out *in vitro* migration and invasion assays. The results represent means of three experiments. $^{*}P < 0.05$ *versus* control (non-specific siRNA). (d,e) HCCLM6 cells were transfected with PKCβ siRNA-1 (70 nM) for 24 h followed by phorbol-12-myristate-13-acetate (20 nM) for 4 h, then subjected to *in vitro* migration (d) and invasion (e) assays for 20 h. The number of migrated and invasive HCCLM6 cells was counted. The results represent means of three experiments. $^{*}P < 0.05$ *versus* vehicle. Similar findings were also observed in metastatic HCC cell clones MHCC97L and MHCC97H (data not shown).

cancer cells,[41] but has also been shown to play an interesting role in tumor angiogenesis.[42,43] In this research concerning HCC, we showed PKCβ's upregulated activation in different metastatic HCC cells (same findings in metastatic HCC tissue compared with non-metastatic HCC tissue, data not shown) and elucidated it's effects on activation of $ERK_{1/2}$ and p38 MAPK and it's lack of effect on activation of JNK. This was indicated through evaluating the inhibitory effects of PKCβ-specific inhibitor LY317615 and PKCβ RNAi combined with PMA stimulation on the phosphorylation levels of three MAPK molecules. However, reports on the effects of PKCβ on ERK, JNK, or p38 MAPK activation are not in agreement with each other in different pathological conditions or different cancers.[37,38] Our findings in HCC cells reveal that both ERK and p38 MAPK are downstream signal molecules of PKCβ and could be effectively activated by PKCβ.

It has also been reported that the MAPK cascade, in particular p38 MAPK, phosphorylates HSP27 through MAPK-activated protein kinase-2, one of the substrates of p38 MAPK.[44] Therefore, we investigated whether MAPKs are involved in HSP27 phosphorylation in our HCC cells. We showed that inhibition of p38 MAPK and $ERK_{1/2}$ activation resulted in the suppression of HSP27 phosphorylation. It was also found that inhibition of PKCβ activation and PKCβ knockdown reduced the phosphorylation level of HSP27 in these HCC cells, and inhibition of p38 MAPK and $ERK_{1/2}$ activation suppressed PMA-stimulated HSP27 phosphorylation. Taking these findings into account, it is most likely that activation of PKC regulates the phosphorylation of HSP27 through $ERK_{1/2}$ and p38 MAPK in human HCC cells. Furthermore, our previous studies raised the possibility that attenuated HSP27 correlates with tumor progression in HCC patients,[45,46] which seems to be in accordance with some studies,[22,47] but the molecular mechanism is still unclear. For these reasons, we further evaluated basal levels of HSP27 and it's phosphorylation in MHCC97L, MHCC97H, and HCCLM6 cells. This result showed consecutively increased basal phosphorylation levels of HSP27 in different metastatic HCC cells and indicates that HSP27 activation is in agreement with HCC cells metastatic potentials.

Collectively, these results suggest consistent activation of the PKCβ–$ERK_{1/2}$/p38 MAPK–HSP27 pathway in our HCC cells and led us to speculate that the pathway plays an important role in HCC metastasis.

In tumor cells, stimulation by various signals that regulate morphology, proliferation, differentiation, or survival often leads to the sequential phosphorylation and activation of at least one member of the MAPK family.[25,26,34] Many studies have identified that MAPK cascades are major signal pathways for driving tumor cell metastasis, mediated by PKC, transforming growth factor β/Smad, and integrin-mediated signaling.[48–50] In this study, the observation that inhibition of PKCβ activation or depletion of PKCβ resulted in decreasing HCC cell motility and invasive ability indicates PKCβ plays a crucial role in HCC cell motility and invasion. This result is in accordance with a report that PKCβ accounts for increased invasion and proliferation rates of intestinal cancer cells.[51] Furthermore, findings that PMA stimulation increased HCC cell motility and invasion, but that HCC cell motility and invasion was significantly reduced with PMA stimulation after depletion of PKCβ, and no statistical difference versus depletion of PKCβ alone, reveal a prominent role for

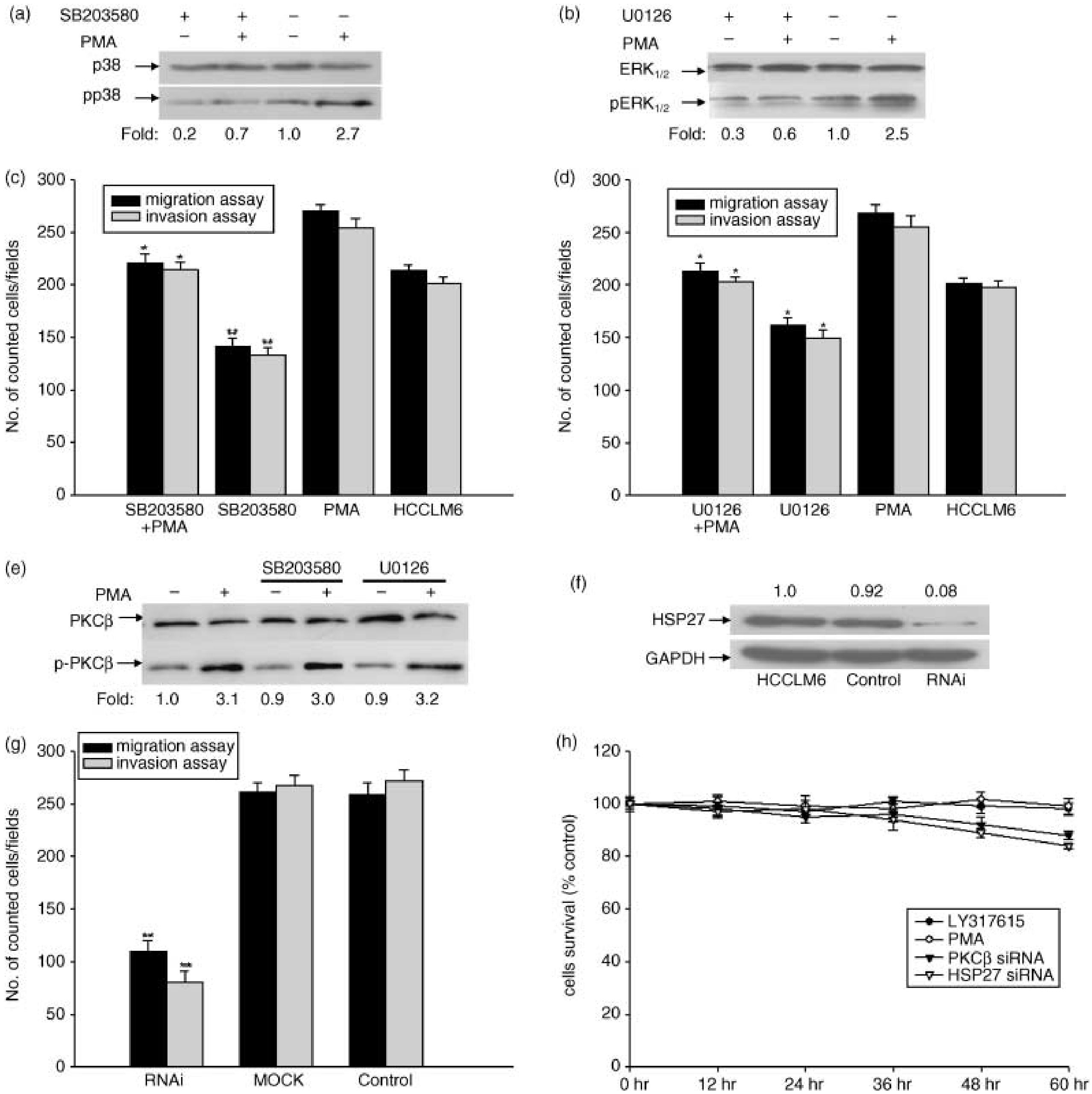

Fig. 6. Protein kinase Cβ (PKCβ)-mediated hepatocellular carcinoma cell motility and invasion depends on activation of extracellular signal-regulating kinase $(ERK)_{1/2}$–heat shock protein 27 (HSP27), and p38 mitogen-activated protein kinase (MAPK)–HSP27. (a, b) HCCLM6 cells were pretreated with 4-(4-Fluorophenyl)-2-(4-methylsulfinylphenyl)-5-(4-pyridyl)1H-imidazole (SB203580; 5 μM) for 2 h or 1.4-diamino-2.3-dicyano-1.4-bis[2-aminophenylthio] butadiene (U0126; 10 μM) for 1.5 h then stimulated by phorbol-12-myristate-13-acetate (PMA; 20 nM) incubation for 4 h. After 20 h, whole cell extracts from these samples were subjected to sodium dodecyl sulfate–polyacrylamide gel electrophoresis (SDS-PAGE). Expression of total $ERK_{1/2}$, p38 MAPK, and their phosphorylated forms were analyzed using specific antibodies by immunoblot analysis. The values underneath the bands represent the densitometric estimation of the relative density of the phosphorylated bands *versus* total protein bands comparing with that of HCCLM6 cells without treatment. (c,d) For observing the effects of SB203580 (c) and U0126 (d) on the migration and invasive ability of PMA-stimulated HCCLM6 cells, *in vitro* migration and invasion assays were carried out in HCCLM6 cells, with the treatment outlined above, for 20 h in the presence of compounds described. The results represent means of three experiments. *$P < 0.05$ *versus* PMA-treated HCCLM6 cells; **$P < 0.01$ *versus* HCCLM6 cells without treatment. (e) HCCLM6 cells were pretreated with U0126 (10 μM) or SB203580 (5 μM) followed by PMA (20 nM) for the indicated times. The blots were analyzed using a specific antibody against PKCβ and phosphor-PKCβ. The values underneath the bands represent the densitometric estimation of the relative density of the phosphorylated bands comparing with that of HCCLM6 cells without treatment. (f) HCCLM6 cells were transfected with HSP27 small interfering RNA (siRNA) and negative control (non-specific siRNA) for 48 h, equal amounts of cell extracts (30 μg) were subjected to SDS-PAGE, the levels of total HSP27 was determined by immunoblot analysis. The level of glyceraldehyde-3-phosphate dehydrogenase (GAPDH) served as the loading control. The values underneath the bands represent the densitometric estimation of the relative density of the band, calculated by comparing the ratio of HSP27 *versus* GAPDH with that of HCCLM6 cells without siRNA treatment (the ratio in HCCLM6 cells without siRNA treatment was set as baseline 1.0). (g) After pretreatment with 100 nM HSP27 siRNA for 12 h, HCCLM6 cells were stimulated by PMA (20 nM) for 4 h then subjected to *in vitro* migration and invasion assays for 20 h. Non-specific siRNA served as a control. The results represent means of three experiments. **$P < 0.01$ *versus* control. (h) HCCLM6 cells in a 96-well plate were treated with 0.025 μM LY317615 or 20 nM PMA, 70 nM PKCβ siRNA, or 100 nM HSP27 for the indicated times. Cell survival was determined by 3-(4,5-dimethylthiazol-2-yl)-2,5-diphenyltetrazolium bromide assay. The results presented are means of three experiments; bars, ±SE.

doi: 10.1111/j.1349-7006.2007.00702.x

PKCβ in HCC cell motility and invasion, compared with other PKC isozymes. The findings also indicate that the effects of PMA on HCC cell motility and invasion depends mainly on PKCβ. Hence, we next addressed the role of $ERK_{1/2}$ and p38 MAPK activation in PMA-stimulated HCC cell motility and invasion. The observation that increase of PMA-induced HCC cell motility and invasion was efficiently negated by inhibition of $ERK_{1/2}$ and p38 MAPK pathway activation suggests that both $ERK_{1/2}$ and p38 MAPK pathways are necessary to maintain PKCβ-mediated HCC cell motility and invasion capacity, and also implies an overlapping function of p38 MAPK and $ERK_{1/2}$ signaling pathways in the regulation of HCC cell motility and invasion. In addition, it was verified that HSP27 knockdown decreased PMA-stimulated HCC cell motility and invasion, suggesting the involvement of HSP27 in PMA-stimulated PKCβ–$ERK_{1/2}$/p38 MAPK-mediated HCC cell motility and invasion. Based on these findings, it is speculated that increased PKCβ phosphorylation might promote HCC metastasis through regulating activation of the $ERK_{1/2}$ and p38 MAPK pathways, verified to phosphorylate HSP27. Further investigations would be required to clarify the detailed mechanism of PKCβ–$ERK_{1/2}$/p38 MAPK–HSP27 activation in human HCC cells.

In summary, our current findings represent a broader extension of the relationship between the MAPK pathway and tumor progression. This illustration of the role of the PKCβ–$ERK_{1/2}$/p38 MAPK–HSP27 pathway in HCC cells enriches the classical p38 MAPK–MAPKK2–HSP27 pathway. Defining the functional significance of this new pathway in HCC metastasis will provide some fundamental information that contributes to the manifestation of HCC cells' metastatic phenotype and finding some potential antimetastasis therapeutic targets in HCC.

Acknowledgments

This work was financially supported by the National High-Tech Program of China (2002-BAC11A11), National Basic Research Priorities Program of China (001CB510205 and 2004CB520802), and the National Natural Science Foundation (3017416).

References

1 Budhu AS, Zipser B, Forgues M, Ye QH, Sun Z, Wang XW. The molecular signature of metastases of human hepatocellular carcinoma. *Oncology* 2005; **69**: 23–7.
2 Chambers AF, MacDonald IC, Schmidt EE, Morris VL, Groom AC. Clinical targets for anti-metastasis therapy. *Adv Cancer Res* 2000; **79**: 91–121.
3 Tang ZY. Hepatocellular carcinoma surgery – review of the past and prospects for the 21st century. *J Surg Oncol* 2005; **91**: 95–6.
4 Christofori G. New signals from the invasive front. *Nature* 2006; **441**: 444–50.
5 Wieser R. The transforming growth factor-beta signaling pathway in tumorigenesis. *Curr Opin Oncol* 2001; **13**: 70–7.
6 Yoshimura A. Signal transduction of inflammatory cytokines and tumor development. *Cancer Sci* 2006; **97**: 439–47.
7 Webb CP, Van Aelst L, Wigler MH, Woude GF. Signaling pathways in Ras-mediated tumorigenicity and metastasis. *Proc Natl Acad Sci USA* 1998; **95**: 8773–8.
8 Tanaka S, Sugimachi K, Kawaguchi H, Saeki H, Ohno S, Wands JR. Grb7 signal transduction protein mediates metastatic progression of esophageal carcinoma. *J Cell Physiol* 2000; **183**: 411–15.
9 Li Y, Tian B, Yang J *et al*. Stepwise metastatic human hepatocellular carcinoma cell model system with multiple metastatic potentials established through consecutive *in vivo* selection and studies on metastatic characteristics. *J Cancer Res Clin Oncol* 2004; **130**: 460–8.
10 Li Y, Tang ZY, Ye SL *et al*. Establishment of cell clones with different metastatic potential from the metastatic hepatocellular carcinoma cell line MHCC97. *World J Gastroenterol* 2001; **7**: 630–6.
11 Mao X, Cai T, Olyarchuk JG, Wei L. Automated genome annotation and pathway identification using the KEGG Orthology (KO) as a controlled vocabulary. *Bioinformatics* 2005; **21**: 3787–93.
12 Wu J, Mao X, Cai T, Luo J, Wei L. KOBAS server: a web-based platform for automated annotation and pathway identification. *Nucleic Acids Res* 2006; **34**: 720–4.
13 Weston CR, Lambright DG, Davis RJ. Signal transduction. MAP kinase signaling specificity. *Science* 2002; **296**: 2345–7.
14 Dunn KL, Espino PS, Drobic B, He S, Davie JR. The Ras–MAPK signal transduction pathway, cancer and chromatin remodeling. *Biochem Cell Biol* 2005; **83**: 1–14.
15 Noguchi T, Metz R, Chen L, Matte MG, Carrasco D, Bravo R. Structure, mapping, and expression of erp, a growth factor-inducible gene encoding a nontransmembrane protein tyrosine phosphatase, and effect of ERP on cell growth. *Mol Cell Biol* 1993; **13**: 5195–205.
16 Rizvi MA, Ghias K, Davies KM *et al*. Enzastaurin (LY317615), a protein kinase Cbeta inhibitor, inhibits the AKT pathway and induces apoptosis in multiple myeloma cell lines. *Mol Cancer Ther* 2006; **5**: 1783–9.
17 Graff JR, McNulty AM, Hanna KR *et al*. The protein kinase Cbeta-selective inhibitor, Enzastaurin (LY317615.HCl), suppresses signaling through the AKT pathway, induces apoptosis, and suppresses growth of human colon cancer and glioblastoma xenografts. *Cancer Res* 2005; **65**: 7462–9.
18 Koivunen J, Aaltonen V, Peltonen J. Protein kinase C (PKC) family in cancer progression. *Cancer Lett* 2006; **235**: 1–10.
19 Miron T, Vancompernolle K, Vandekerckhove J, Wilchek M, Geiger B. A 25-kD inhibitor of actin polymerization is a low molecular mass heat shock protein. *J Cell Biol* 1991; **114**: 255–61.
20 Hino M, Kurogi K, Okubo MA, Murata-Hori M, Hosoya H. Small heat shock protein 27 (HSP27) associates with tubulin/microtubules in HeLa cells. *Biochem Biophys Res Commun* 2000; **271**: 164–9.
21 Kyriakis JM, Avruch J. Sounding the alarm: protein kinase cascades activated by stress and inflammation. *J Biol Chem* 1996; **271**: 24313–16.
22 Guay J, Lambert H, Gingras-Breton G, Lavoie JN, Huot J, Landry J. Regulation of actin filament dynamics by p38 MAP kinase-mediated phosphorylation of heat shock protein 27. *J Cell Sci* 1997; **110**: 357–68.
23 Benjamin IJ, McMillan DR. Stress (heat shock) proteins: molecular chaperones in cardiovascular biology and disease. *Circ Res* 1998; **83**: 117–32.
24 Park KJ, Gaynor RB, Kwak YT. Heat shock protein 27 association with the I kappa B kinase complex regulates tumor necrosis factor alpha-induced NF-kappa B activation. *J Biol Chem* 2003; **278**: 35272–8.
25 Fang JY, Richardson BC. The MAPK signalling pathways and colorectal cancer. *Lancet Oncol* 2005; **6**: 322–7.
26 Murphy LO, Blenis J. MAPK signal specificity: the right place at the right time. *Trends Biochem Sci* 2006; **31**: 268–75.
27 Boldt S, Weidle UH, Kolch W. The role of MAPK pathways in the action of chemotherapeutic drugs. *Carcinogenesis* 2002; **23**: 1831–8.
28 Bradham C, McClay DR. p38 MAPK in development and cancer. *Cell Cycle* 2006; **5**: 824–8.
29 Behren A, Binder K, Vucelic G *et al*. The p38 SAPK pathway is required for Ha-ras induced *in vitro* invasion of NIH3T3 cells. *Exp Cell Res* 2005; **303**: 321–30.
30 Lee KH, Hyun MS, Kim JR. Growth factor-dependent activation of the MAPK pathway in human pancreatic cancer: MEK/ERK and p38 MAP kinase interaction in uPA synthesis. *Clin Exp Metastasis* 2003; **20**: 499–505.
31 Tsuda H, Sata M, Kumabe T, Uchida M, Hara H. The preventive effect of antineoplaston AS2-1 on HCC recurrence. *Oncol Rep* 2003; **10**: 391–7.
32 Ou DP, Yang LY, Huang GW, Tao YM, Ding X, Chang ZG. Clinical analysis of the risk factors for recurrence of HCC and its relationship with HBV. *World J Gastroenterol* 2005; **11**: 2061–6.
33 Zeng ZC, Tang ZY, Fan J *et al*. Consideration of role of radiotherapy for lymph node metastases in patients with HCC: retrospective analysis for prognostic factors from 125 patients. *Int J Radiat Oncol Biol Phys* 2005; **63**: 1067–76.
34 Qi M, Elion EA. MAP kinase pathways. *J Cell Sci* 2005; **118**: 3569–72.
35 Ito Y, Sasaki Y, Horimoto M *et al*. Activation of mitogen-activated protein kinases/extracellular signal-regulated kinases in human hepatocellular carcinoma. *Hepatology* 1998; **27**: 951–8.
36 Cuevas BD, Abell AN, Johnson GL. Role of mitogen-activated protein kinase kinase kinases in signal integration. *Oncogene* 2007; **26**: 3159–71.
37 Fujita T, Asai T, Andrassy M *et al*. PKCbeta regulates ischemia/reperfusion injury in the lung. *J Clin Invest* 2004; **113**: 1615–23.
38 Troller U, Zeidman R, Svensson K, Larsson C. A PKCbeta isoform mediates phorbol ester-induced activation of Erk1/2 and expression of neuronal differentiation genes in neuroblastoma cells. *FEBS Lett* 2001; **508**: 126–30.
39 Chiarini A, Whitfield JF, Armato U, Dal Pra I. Protein kinase C-beta II Is an apoptotic lamin kinase in polyomavirus-transformed, etoposide-treated pyF111 rat fibroblasts. *J Biol Chem* 2002; **277**: 18827–39.
40 Kawakami T, Kawakami Y, Kitaura J. Protein kinase C beta (PKC beta): normal functions and diseases. *J Biochem* 2002; **132**: 677–82.
41 Larsson C. Protein kinase C and the regulation of the actin cytoskeleton. *Cell Signal* 2006; **18**: 276–84.

42 Oka M, Kikkawa U. Protein kinase C in melanoma. *Cancer Metastasis Rev* 2005; **24**: 287–300.
43 Park IC, Park MJ, Rhee CH *et al*. Protein kinase C activation by PMA rapidly induces apoptosis through caspase-3/CPP32 and serine protease(s) in a gastric cancer cell line. *Int J Oncol* 2001; **18**: 1077–83.
44 Landry J, Lambert H, Zhou M *et al*. Human HSP27 is phosphorylated at serines 78 and 82 by heat shock and mitogen-activated kinases that recognize the same amino acid motif as S6 kinase II. *J Biol Chem* 1992; **267**: 794–803.
45 Feng JT, Liu YK, Song HY *et al*. Heat-shock protein 27: a potential biomarker for hepatocellular carcinoma identified by serum proteome analysis. *Proteomics* 2005; **5**: 4581–8.
46 Song HY, Liu YK, Feng JT *et al*. Proteomic analysis on metastasis-associated proteins of human hepatocellular carcinoma tissues. *J Cancer Res Clin Oncol* 2006; **132**: 92–8.
47 Ciocca DR, Vargas-Roig LM. Hsp27 as a prognostic and predictive factor in cancer. *Prog Mol Subcell Biol* 2002; **28**: 205–18.
48 ten Dijke P, Hill CS. New insights into TGF-beta-Smad signalling. *Trends Biochem Sci* 2004; **29**: 265–73.
49 Vo HP, Lee MK, Crowe DL. Alpha2beta1 integrin signaling via the mitogen activated protein kinase pathway modulates retinoic acid-dependent tumor cell invasion and transcriptional downregulation of matrix metalloproteinase 9 activity. *Int J Oncol* 1998; **13**: 1127–34.
50 Aikawa R, Nagai T, Kudoh S *et al*. Integrins play a critical role in mechanical stress-induced p38 MAPK activation. *Hypertension* 2002; **39**: 233–8.
51 Zhang J, Anastasiadis PZ, Liu Y, Thompson EA, Fields AP. Protein kinase C (PKC) betaII induces cell invasion through a Ras/Mek-, PKC iota/Rac 1-dependent signaling pathway. *J Biol Chem* 2004; **279**: 22118–23.

doi: 10.1111/j.1349-7006.2007.00702.x